Iron(II) complexes with novel pentadentate ligands *via* C−C bond formation between various nitriles and [2,4-bis(2-pyridylmethyl-imino)pentane]iron(II) perchlorate: synthesis and structures ‡

Masafumi Goto,*†,[a] Yoshinobu Ishikawa,[a] Takao Ishihara,[a] Chika Nakatake,[a] Tomoe Higuchi,[a] Hiromasa Kurosaki[a] and (the late) Virgil L. Goedken[b]

[a] *Faculty of Pharmaceutical Sciences, Kumamoto University, 5-1 Oe-honmachi, Kumamoto, 862, Japan*
[b] *Department of Chemistry, Florida State University, Talahassee, Florida, USA*

The iron(II) complex of 2,4-bis(2-pyridylmethylimino)pentane (L^1), *trans*-[FeL^1(MeCN)$_2$][ClO$_4$]$_2$·MeCN, was prepared by a template reaction and isolated as pale red crystals. An acetonitrile solution of the complex exhibited a crossover from a low- to a high-spin form above 20 °C. With this complex as precursor, a series of iron(II) complexes with novel pentadentate ligands, 3-(1-alkyl (or aryl)-methyl)-1-imino-2,4-bis(2-pyridylmethylimine) (L^2), was prepared using various nitriles such as propionitrile, isobutyronitrile, benzyl cyanide, benzonitrile, 4-fluoro-, 3,4-difluoro-, and pentafluoro-benzonitrile, as well as acetonitrile, as solvents. On formation of L^2, the co-ordination mode of the L^1 part of the parent compound was converted from *trans* into *cis*-β with concomitant C−C bond formation between the central carbon atom of L^1 and the carbon atom of the various nitriles. The isolated triimine part in the pentadentate ligands occupies one of the trigonal faces of the distorted octahedron. The resulting complex undergoes rapid intramolecular isomerization at or above room temperature. The crystal structures of the precursor and of three new iron(II) complexes with pentadentate ligands have been determined.

Much current research centres on iron complexes with macrocyclic polyamines and polyimines including porphyrins and with tripodal ligands, but less is known about iron(II) complexes with linear tetradentate ligands,[1] albeit that the high-spin iron(II) complex of H$_2$salen, *N*,*N'*-bis(salicylidene)ethane-1,2-diamine, was reported as early as 1968.[2] The chemistry of iron(II) complexes with linear polyamines or polyimines is expected to be more complicated than those with macrocyclic ones because the isomerism is more complicated and the flexibility of the structure is enhanced.

As regards the donor groups, pyridine has an advantage in as much as it provides a nitrogen atom resistant to dehydrogenation at the primary or secondary amine site[3] of low-spin polyamine iron(II) complexes, which leads to mixtures too complicated to handle without careful and constant scrutiny of the design of the ligand.[4]

Bis(2-pyridylmethyl)amine,[5] tris(2-pyridylmethyl)amine,[6,7] and *N*,*N*,*N'*,*N'*-tetrakis(2-pyridylmethyl)ethane-1,2-diamine[8,9] were employed in order to reveal new aspects of iron-(II) and -(III) complexes.

The enhanced reactivity of co-ordinated nitriles toward nucleophiles has been investigated extensively,[10] since they are endowed with Lewis acidity from the metal ions. The remarkable formation of a C−C bond between co-ordinated acetonitrile and a macrocyclic imine in iron(II) complexes has been reported by Busch, Riley and co-workers.[11–13] In this reaction, a 1,3-diimine group is the key to the structure because it provides a nucleophile on deprotonation. This reaction is intriguing for increasing the co-ordination number from four to either five or six. Similar reactions with acetonitrile and acetylene were reported for a cobalt(III) complex of another macrocyclic tetraimine, tetraaza[14]annulene, containing a 1,3-diimine group.[14]

In this paper we describe a new iron complex of a tetradentate ligand, L^1, containing a 1,3-diimine group flanked by 2-pyridylmethyl moieties, and which is formally derived from

L^1
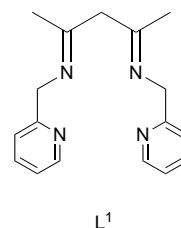
pentane-2,4-dione and 2-aminomethylpyridine. This ligand was previously exploited in the evaluation of the oxygenation ability of a cobalt(II) complex, but its structure was not investigated in detail.[15]

The synthesis of the iron(II) complex of this ligand and its reaction products with several nitriles are reported as are their structures, obtained by X-ray crytallography, and spectroscopic properties. A preliminary communication of this work has recently been published.[16]

Experimental

Materials

Iron(II) perchlorate hexahydrate was obtained from Alfa and used as supplied, acetonitrile, ethyl orthoformate, pentane-2,4-dione and 2-aminomethylpyridine from Wako. Acetonitrile was twice distilled over CaH$_2$, ethyl orthoformate under reduced pressure (b.p. 56.5 °C, 29 mmHg), pentane-2,4-dione over NaHCO$_3$ and redistilled over P$_2$O$_5$ under reduced pressure and 2-aminomethylpyridine after dehydration with NaOH. Benzonitrile, propionitrile, phenylacetonitrile(benzyl cyanide), isobutyronitrile, trimethylacetonitrile(pivalonitrile), 4-fluorobenzonitrile, 3,4-difluorobenzonitrile and pentafluorobenzonitrile from Tokyo Kasei were used after dehydration with molecular sieve 4A. Triethylamine and tetra(*n*-butyl)ammonium perchlorate were obtained from Nakalai. Diethyl ether was distilled over LiAlH$_4$ after prior dehydration with CaH$_2$, thf over sodium–benzophenone and triethylamine after dehydration with CaH$_2$.

† E-Mail: gotomphi@gpo.kumamoto-u.ac.jp
‡ *Non-SI unit employed:* mm Hg ≈ 133 Pa, µ$_B$ ≈ 9.27 × 10^{-24} J T^{-1}.

Preparations

4-Oxo-2-pentylidene-2-pyridylmethanamine. A mixture of pentane-2,4-dione (16.8 g, 0.168 mol) and 2-aminomethylpyridine (20.0 g, 0.185 mol) in ethyl orthoformate (250 cm³, 1.50 mol) was refluxed at 100 °C overnight. The resultant mixture was distilled to remove pentane-2,4-dione (45 °C, 30 mmHg), ethyl orthoformate (56.5 °C, 29 mmHg) and 2-aminomethylpyridine (86–87 °C, 14 mmHg). A yellow oil was obtained as a pure product by distillation from the remaining mixture. Yield 24.7 g (77.4%), b.p. 145 °C (4 mmHg). NMR (CDCl₃) (enol form predominant): [1]H (400 MHz), δ 1.94 (3 H, s, CH₃), 2.05 (3 H, s, CH₃), 4.60 (2 H, d, $J = 6.6$, CH₂), 5.08 (1 H, s, CH), 7.20 (1 H, dd, $J = 4.9$ and 7.7, H5), 7.28 (1 H, d, $J = 6.6$, H3), 7.68 (1 H, dd, $J = 6.6$ and 7.7, H4), 8.57 (1 H, d, $J = 4.8$ Hz, H6) and 11.28 (1 H, s, OH).

trans-[FeL^1(MeCN)₂][ClO₄]₂·MeCN 1. This compound was prepared as described previously.[16]

Nitrile adducts of complex 1. The chemical shifts for the ^{1}H signals of CD₃CN solutions at −35 °C common to complexes **2a**–**2h** (**2s**) are in Table 1.

(*Acetonitrile*) [3-(1-*iminoethyl*)-2,4-*bis*(2-*pyridylmethylimino*)-*pentane*]*iron*(II) *perchlorate–tetrahydrofuran* (1/1), [FeL^{2a}-(MeCN)][ClO₄]₂·thf **2a**. This compound was prepared as described previously.[16] ^{13}C and ^{1}H NMR based on HMQC at −10 °C: C(1), δ 152.51; C(2), 125.03; C(3), 138.90; C(4), 121.92; C(5), 165.70; C(6), 61.06; C(7), 176.96; C(8), 69.35; C(9), 177.78; C(10), 60.39; C(11), 165.13; C(12), 122.60; C(13), 139.19; C(14), 125.27; C(15), 156.01; C(16), 24.39; C(17), 24.28; C(18), 184.70; and C(19), 29.15; H(1), 7.10 (d, $J = 5.5$); H(2), 7.18 (t, $J = 6.4$); H(3), 7.82 (t, $J = 7.3$); H(4), 7.50 (d, $J = 8.3$); H(5), 5.25 (d, $J = 17.4$); H(6), 5.48 (d, $J = 17.4$); H(7), 5.68 (d, $J = 1.8$); H(8), 5.33 (d, $J = 17.4$); H(9), 4.82 (d, $J = 18.3$), H(10), 7.64 (d, $J = 8.3$); H(11), 8.01 (t, $J = 7.3$); H(12), 7.57 (t, $J = 6.4$); H(13), 9.03 (d, $J = 5.5$); H(14)–H(16), 2.57 (s); H(17)–H(19), 2.42 (s); H(20), 11.23 (s); and H(21)–H(23), 2.51 (s).

[²H₃]*Acetonitrile adduct*, [FeL$^{2a'}$(MeCN)][ClO₄]₂·thf **2a′**. The above method was followed except for the use of CD₃CN instead of acetonitrile. Yield 106 mg (67.2%) (Found: C, 43.53; H, 4.96; N, 11.89. Calc. for C₂₁[1]H₂₃²H₃Cl₂FeN₆O₈·C₄H₈O: C, 43.37; H, 5.39; N, 12.14%).

(*Acetonitrile*) [3-(1-*iminopropyl*)-2,4-*bis*(2-*pyridylmethylimino*)*pentane*]*iron*(II) *perchlorate–tetrahydrofuran* (1/1) [FeL^{2b}-(MeCN)][ClO₄]₂·thf **2b**. In a Schlenk flask complex **1** (240 mg, 3.65×10^{-4} mol) was dissolved in propionitrile (7 cm³). To the resultant red solution five drops of triethylamine were added through a syringe at room temperature. After stirring for 2 h the solution was concentrated under vacuum, dissolved in acetonitrile (5 cm³) and filtered. To the filtrate, thf (35 cm³) was added and the mixture allowed to stand at room temperature. This gave brown needles that were collected in a filter, washed with ether (10 cm³) and dried. Yield 145 mg (56.5%) (Found: C, 44.14; H, 5.07; N, 12.13. Calc. for C₂₂H₂₈Cl₂FeN₆O₈·C₄H₈O: C, 44.40; H, 5.16; N, 11.95%). Selected IR: ν(N–H) 3242 and 3262 cm⁻¹. ^{1}H NMR: δ 1.11 (t, 3 H) and 2.73 (q, 2 H).

(*Acetonitrile*)[3-(1-*imino-2-methylpropyl*)-2,4-*bis*(2-*pyridylmethylimino*)*pentane*]*iron*(II) *perchlorate–tetrahydrofuran* (1/1), [FeL^{2c}(MeCN)][ClO₄]₂·thf **2c**. The method used was similar to that described above using complex **1** (294 mg, 4.47×10^{-4} mol) and isobutyronitrile (7 cm³) for 2.5 h. Yield 82 mg (26%) (Found: C, 45.23; H, 5.41; N, 11.64. Calc. for C₂₃H₃₀-Cl₂FeN₆O₈·C₄H₈O: C, 45.21; H, 5.34; N, 11.72%). Selected IR: ν(N–H) 3254 cm⁻¹. ^{1}H NMR: δ 1.12 (d, 6 H) and 2.96 (m, 1 H).

(*Acetonitrile*)[3-(1-*imino-2-phenylethyl*)-2,4-*bis*(2-*pyridylmethylimino*)]*iron*(II) *perchlorate–tetrahydrofuran* (1/1) [FeL^{2d}-(MeCN)][ClO₄]₂·thf **2d**. The method was similar to that described above, using complex **1** (213 mg, 3.24×10^{-4} mol) and

benzyl cyanide (6 cm³) for 2 h. Yield 157 mg (63.4%) (Found: C, 48.30; H, 4.96; N, 10.99. Calc. for C₂₇H₃₀Cl₂FeN₆O₈·C₄H₈O: C, 48.65; H, 5.00; N, 10.98%). Selected IR: ν(N–H) 3240 and 3262 cm⁻¹. ^{1}H NMR: 4.08 (d, 2 H) and 7.35–7.45 (m, 5 H).

(*Acetonitrile*)[3-[1-*imino-1-phenylmethyl*]-2,4-*bis*(2-*pyridyl-methylimino*)*pentane*]*iron*(II) *perchlorate–tetrahydrofuran* (2/1), [FeL^{2e}(MeCN)][ClO₄]₂·0.5thf **2e**. The method was similar to that described above using complex **1** (462 mg, 7.02×10^{-4} mol) and benzonitrile (8 cm³) for several minutes. Yield 396 mg (78.9%) (Found: C, 46.74; H, 4.55; N, 12.03. Calc. for C₂₆H₂₈-Cl₂FeN₆O₈·0.5C₄H₈O: C, 47.01; H, 4.51; N, 11.75%). Selected IR: ν(N–H) 3262 cm⁻¹. ^{1}H NMR: δ 7.50–7.80 (m, 5 H).

(*Acetonitrile*){3-[1-(4-*fluorophenyl*)-1-*iminomethyl*]-2,4-*bis*-(2-*pyridylmethylimino*)*pentane*}*iron*(II) *perchlorate–tetrahydro-furan* (2/1), [FeL^{2f}(MeCN)][ClO₄]₂·0.5thf **2f**. Complex **1** (286 mg, 4.34×10^{-4} mol) was dissolved in 4-fluorobenzonitrile (5 cm³) and the mixture warmed to 40 °C. Five drops of triethylamine were added to the red solution and the mixture was stirred for 0.5 h at 40 °C. The addition of ether (40 cm³) caused an orange powder to be precipitated. The ether layer was removed and the residue dried *in vacuo*. Acetonitrile (5 cm³) was added to dissolve the powder followed by thf (40 cm³) and the mixture kept at −20 °C overnight. Orange crystals separated, and were filtered off, washed with ether (10 cm³, three times) and dried *in vacuo*. Yield 265 mg (83.2%) (Found: C, 45.71; H, 4.56; N, 11.33. Calc. for C₂₆H₂₇Cl₂FFeN₆O₈·0.5C₄H₈O: C, 45.86; H, 4.26; N, 11.46%). Selected IR: ν(N–H) 3270 cm⁻¹.

(*Acetonitrile*){3-[1-(3,4-*difluorophenyl*)-1-*iminomethyl*]-2,4-*bis*(2-*pyridylmethylimino*)*pentane*}*iron*(II) *perchlorate–hydrate–diethyl ether* (2/1/1), [FeL^{2g}(MeCN)][ClO₄]₂·0.5H₂O·0.5OEt₂ **2g**. The method was similar to that described above, using complex **1** (330 mg, 5.01×10^{-4} mol) and 3,4-difluorobenzonitrile (1.7 cm³). The mixture was stirred at room temperature for 30 min. Yield 299 mg (78.3%) (Found: C, 43.85; H, 4.48; N, 11.41. Calc. for C₂₆H₂₆Cl₂F₂FeN₆O₈·0.5H₂O·0.5C₄H₁₀O: C, 44.17; H, 4.24; N, 11.04%). Selected IR: ν(N–H) 3256 cm⁻¹.

(*Acetonitrile*)[3-(1-*imino-1-pentafluorophenylmethyl*)-2,4-*bis*(2-*pyridylmethylimino*)*pentane*]*iron*(II) *perchlorate*, [FeL^{2h}-(MeCN)][ClO₄]₂ **2h**. The method was similar to that described above, using complex **1** (496 mg, 7.53×10^{-4} mol) and penta-fluorobenzonitrile (8 cm³) for 10 min. Yield 282 mg (49%) (Found: C, 40.88; H, 3.01; N, 10.77. Calc. for C₂₆H₂₃Cl₂-F₅FeN₆O₈: C, 40.60; H, 3.01; N, 10.93%). Selected IR: ν(N–H) 3263 cm⁻¹.

X-Ray crystallography

Complex 1. A red prism was picked from the crystals of the reaction product, placed on a vessel under an argon atmosphere, swiftly covered with epoxy resin as the crystals were sensitive to air and moisture, and mounted on a capillary. The measurements of the crystallographic data and the collection of reflection intensities were carried out with a Rigaku AFC7R diffractometer. The structure was solved by the direct method with the TEXSAN package[17] on a Iris-Indigo work station.

Complex 2a. An orange prism was mounted on a glass capillary. The measurement procedure and the analysis was carried out as described above. All the non-hydrogen atoms were refined with anisotropic thermal factors. Hydrogen atoms were placed at calculated positions with isotropic thermal factors. The perchlorates and thf are possibly disordered, however any disordered structural model failed to improve the agreement between calculated and observed reflections. The oxygen atoms of thf molecules were placed at the positions where the thermal parameters were smallest.

[FeL^{2d}(MeCN)][PF₆]₂·Me₂CO and 2e. The anion of complex **2d** was converted into hexafluorophosphate by adding a large excess of ammonium hexafluorophosphate in acetone–

Table 1 Comparison of ^{1}H chemical shifts (δ) of the nitrile adducts **2** at −35 °C in CD$_3$CN

Complex	H(1)	H(2)	H(3)	H(4)	H(5)	H(6)	H(7)	H(8)	H(9)	H(10)	H(11)	H(12)	H(13)	H(20)	H(14)–H(16)	H(17)–H(19)
2a	7.10	7.18	7.82	7.49	5.39	5.24	5.66	5.33	4.79	7.63	8.02	7.57	9.03	11.14	2.58	2.40
2b	7.07	7.17	7.82	7.49	5.49	5.24	5.70	5.34	4.80	7.64	8.02	7.57	9.07	11.04	2.54	2.39
2c	7.05	7.17	7.82	7.49	5.48	5.24	5.82	5.34	4.81	7.65	8.03	7.57	9.07	11.08	2.54	2.39
2d	7.06	7.17	7.81	7.46	5.39	5.20	5.45	5.31	4.77	7.64	8.04	7.58	9.03	11.34	2.14	2.10
2e	7.13	7.23	7.86	7.53	5.55	5.26	6.37	5.35	4.87	7.65	8.05	7.60	9.12	12.15	2.63	2.43
2f	7.13	7.22	7.86	7.54	5.54	5.25	6.32	5.34	4.86	7.65	8.05	7.60	9.11	12.10	2.62	2.41
2g	7.13	7.23	7.87	7.55	5.55	5.25	6.29	5.33	4.85	7.65	8.05	7.61	9.11	12.30	2.61	2.41
2h	7.12	7.26	7.89	7.57	5.57	5.25	6.03	5.34	4.86	7.68	8.07	7.61	9.06	13.18	2.60	2.44

acetonitrile solution. The crystal data for both complexes were obtained by least-squares fitting of 25 reflection data. The structures were solved by the heavy atom method.[17] In the last cycle of refinement all the hydrogens were placed at calculated positions and the isotropic factors were refined. Crystal data for all the complexes are listed in Table 2.

CCDC reference number 186/883.

See http://www.rsc.org/suppdata/dt/1998/1213/ for crystallographic files in .cif format.

Physical measurements

The UV/VIS absorption spectra were recorded on a Shimadzu UV-2200 spectrophotometer, infrared spectra on a JEOL JIW-6500W FT spectrophotometer with the samples in compressed KBr discs, ^{1}H NMR spectra on JEOL EX-270 and GX-400 spectrometers in CD$_3$CN solution with the tube sealed under vacuum after several freeze–pump–thaw cycles. The ^{1}H-detected heteronuclear multiple-quantum correlation (HMQC)[18] and heteronuclear multiple-bond correlation (HMBC)[19] experiments on complex **2a** were performed on a JEOL α-500 spectrometer equipped with a field-gradient apparatus (the intensities of the field gradient were 6 and 3 mT cm^{-1}) at −10 °C using 30 mg of complex in CD$_3$CN (0.7 cm^3) sealed under vacuum. The HMQC spectrum resulted from a 1024 × 256 data matrix size, with 16 scans per t_1 value (preceded by four dummy scans) and a delay time between scans of 1.5 s, including a 102 ms acquisition time.

Spectral widths of 5000.0 and 31 948.9 Hz were used in the ^{1}H and ^{13}C dimensions respectively. The HMBC spectrum with J values of 8.0 Hz resulted from a 1024 × 256 data matrix with four scans per t_1 value (preceded by four dummy scans) and a delay time between scans of 1.5 s, including a 102.4 ms acquisition time, and were acquired with the same sweep widths as in the HMQC experiment. The HMQC and HMBC spectra were processed with sine bell window functions in both dimensions.

Electrochemistry

Cyclic voltammetry was carried out using a BAS CV-27 voltammograph and a Riken-Denshi F-3EH X-Y recorder. The conventional three-electrode arrangement was used, consisting of a glassy carbon (diameter = 3 mm) working electrode, a Ag–Ag$^+$ reference electrode (NBu$^n_4$ClO$_4$–MeCN) for organic solvents, and a platinum-wire auxiliary electrode. About 1 mmol dm^{-3} acetonitrile solutions of the nitrile adducts with 0.1 mol dm^{-3} NBu$^n_4$ClO$_4$ as supporting electrolyte were used. The redox potential $E°$ and peak separation $\Delta E°$ were estimated from equations (1) and (2), where E_{pa} and E_{pc} are the potentials of the anode and cathode peak respectively.

$$E° = (E_{pa} + E_{pc})/2 \qquad (1)$$

$$\Delta E° = |E_{pa} - E_{pc}| \qquad (2)$$

Magnetic susceptibility

The magnetic susceptibility of complex **1** was measured in [^{2}H$_3$]acetonitrile solution at a concentration of 0.052 mol dm^{-3}
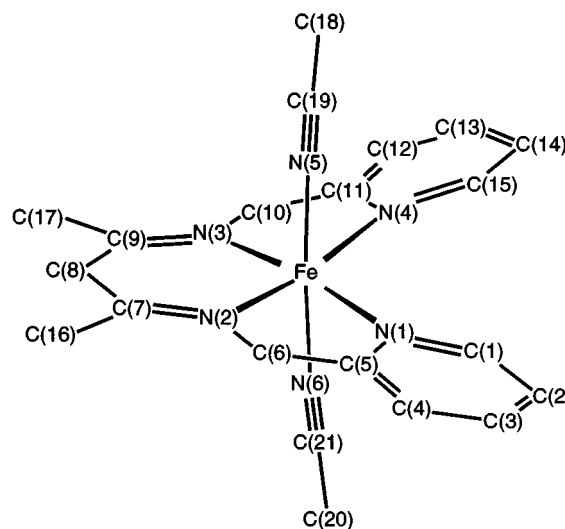
Fig. 1 Schematic drawing of complex **1**

between −30 and 60 °C, by the Evans method[20] using a JEOL EX270 spectrometer. At temperatures higher than 60 °C the ligand reacted with acetonitrile and resulted in imprecise data. Cyclohexane was used as an inert reference. Pascal's constants were used to correct for ligand diamagnetism.[21]

Results

Synthesis of complex 1

Complex **1** was prepared under strict anaerobic and dry conditions by successive additions of the tridentate precursor MeCOCH$_2$C(Me)=NHCH$_2$C$_5$H$_4$N and 2-aminomethylpyridine to an acetonitrile solution of [Fe(MeCN)$_6$]$^{2+}$ prepared *in situ*. Addition of ether to the red solution led to the isolation of crystals of the iron(II) complex in a fair yield (50–60%). These crystals were not stable when exposed to the air and thus were stored under vacuum, and are also potentially explosive. Several attempts to prepare L^1 from a dry mixture of pentane-2,4-dione and 2 equivalents of 2-aminomethylpyridine resulted in the isolation of the tridentate precursor on distillation.

Structure of complex 1

The structure of the red crystals of complex **1** have been reported earlier;[16] selected bond distances and angles are given in Table 3. An schematic drawing of **1** is shown in Fig. 1.

Spectroscopic properties of complex 1

This complex showed a C≡N stretching band at 2244 cm^{-1} (KBr discs) and two weak absorptions at around 720 and 527 nm (ε = 150 dm^3 mol^{-1} cm^{-1}) in acetonitrile solution which are assigned to d–d transitions ($^1A_{1g} \longrightarrow {}^1T_{1g}$). The strong absorption at 358 nm (ε = 8440 dm^3 mol^{-1} cm^{-1}) is ascribed to a metal-to-ligand charge-transfer (MLCT) transition from Fe^{II} to isolated imine and pyridine. When the temperature was raised from 20 to 60 °C in the spectrophotometer cell the absorption

Table 2 Summary of crystallographic data for complexes **1**, **2a**, [FeL²ᵈ(MeCN)][PF₆]₂·Me₂CO and **2e** [a]

Complex	1	2a	[FeL²ᵈ(MeCN)][PF₆]₂·Me₂CO	2e
Formula	$C_{23}H_{29}Cl_2FeN_7O_8$	$C_{25}H_{34}Cl_2FeN_6O_9$	$C_{30}H_{36}F_{12}FeN_6OP_2$	$C_{28}H_{32}Cl_2FeN_6O_{8.5}$
M	658.28	689.33	842.28	715.35
Crystal size/mm	$0.45 \times 0.24 \times 0.15$	$0.60 \times 0.30 \times 0.30$	$0.39 \times 0.15 \times 0.05$	$0.30 \times 0.30 \times 0.15$
Crystal system	Triclinic	Monoclinic	Monoclinic	Monoclinic
Space group	$P\bar{1}$	$P2_1/a$	$P2_1$	$P2_1/n$
a/Å	12.361(3)	19.235(2)	11.027(3)	13.027(4)
b/Å	12.415(2)	16.044(3)	14.571(3)	15.798(3)
c/Å	10.472(2)	20.732(3)	11.562(3)	15.667(2)
α/°	94.68(1)	—	—	—
β/°	112.19(1)	102.91(1)	93.47(2)	94.91(2)
γ/°	80.41(2)	—	—	—
U/Å³	1467.1(6)	6236(1)	1854.3(8)	3212(1)
Z	2	8 [b]	2	4
D_c/g cm⁻³	1.490	1.468	1.509	1.480
μ/mm⁻¹	0.753	0.713	0.587	0.697
$F(000)$	680	2864	860.00	1528.00
Decay (%)	19.0	−1.9	2.6	0.5
hkl Ranges	0 to 16, −16 to 16, −14 to 14	0 to 25, 0 to 21, −27 to 27	0 to 14, 0 to 19, −15 to 15	0 to 17, 0 to 21, −20 to 20
Total data	7060	15 260	4653	7981
Unique data	6742	14 829	4435	7656
Observed data [$I > 3\sigma(I)$]	3399	7115	2956 [c]	3773
Least-squares variables	370	774	468	395
$R[I > 3\sigma(I)]$	0.050	0.082	0.064 [c]	0.064
R' [$I > 3\sigma(I)$]	0.055	0.068	0.055 [c]	0.118
Difference map features/e Å⁻³	+0.53, −0.45	+1.03, −0.68	+0.38, −0.31	+0.87, −0.60

[a] Details in common: Rigaku AFC7R diffractometer, λ(Mo-Kα) = 0.710 69 Å, ω–2θ scan type, $T = 293(1)$ K, $2\theta_{max} = 55.0°$. $R = \Sigma||F_o| - |F_c||/\Sigma|F_o|$; $R' = [\Sigma w(|F_o| - |F_c|)^2/\Sigma wF_o^2)]^{\frac{1}{2}}$, where $w = 1/\sigma^2(F_o) = 4F_o^2/\sigma^2(F_o^2)$. [b] There are two independent molecules in the asymmetric unit. [c] $I > 2\sigma(I)$.

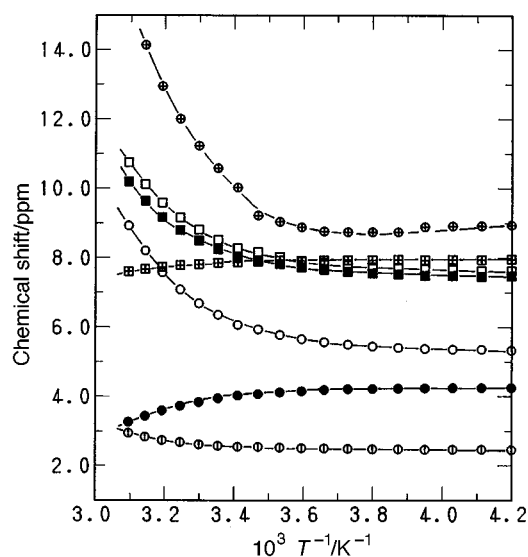**Fig. 2** Variation of ¹H chemical shifts of complex **1** with temperature: ○, $C_5H_4NCH_2$; ●, $C(CH_3)CH_2C(CH_3)$; ◐, $C(CH_3)CH_2C(CH_3)$; ⊕, H(6) of py, □, H(3) of py; ■, H(5) of py, ⊞, H(4) of py

Fig. 3 Proton NMR spectra of a CD₃CN solution of complex **1** at −20 (top) and −60 °C (bottom)

maximum at 527 nm decreased in magnitude by 11%. The ¹H NMR spectrum of this compound exhibited seven signals which obey a non-Curie dependency as shown in Fig. 2. Below 20 °C each signal appeared at the chemical shift expected for an diamagnetic compound but a significant deviation was found above this temperature.

At the lowest extreme with a temperature of −60 °C some signals were separated and others deformed and the number of signals increased to more than seven as shown in Fig. 3, indicating that the *trans* configuration is not fixed in acetonitrile. The molecular fluctuations of iron(II) complexes with pyridylmethyl-substituted polyamines have been reported [9,22] and the mono-(acetonitrile) complex of L²ᵃ described below undergoes rapid isomerization above room temperature.
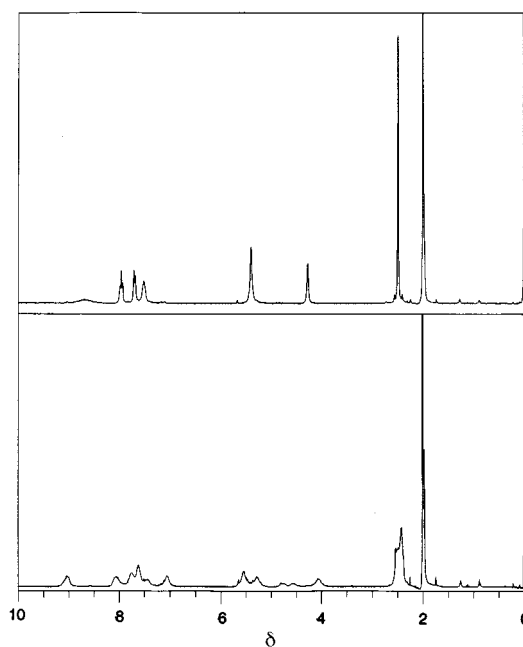
The magnetic susceptibility of an acetonitrile solution of

complex **1** was evaluated by the Evans method.[20] The temperature dependence of the effective magnetic moment, μ_{eff}, is shown in Fig. 4. The equilibrium constants at different temperatures between $^1A_{1g}$ and $^5T_{2g}$ states and the thermodynamic parameters were estimated based on the assumption that the magnetic moments of the high- and low-spin forms are 4.9 and 0.0 μ_B from equations (3) and (4).[23] At temperatures between 20

$$K_{eq} = [\text{high-spin}]/[\text{low-spin}] = \mu_{eff}^2/(24 - \mu_{eff}^2) \quad (3)$$

$$\ln K_{eq} = -(\Delta H/RT) + (\Delta S/R) \quad (4)$$

and 60 °C the van't Hoff plots of ln K_{eq} *vs.* $1/T$ are linear and

Table 3 Comparisons of geometries around Fe^{II} in complexes **1**, **2a**, **2d** and **2e**

			2a			
			Molecule A	B*	2d	2e
			1			
Pyridine N						
	Fe–N(1)	2.006(4)	Fe–N(1)	2.030(8)	2.001(8)	2.010(9)	2.021(5)
	Fe–N(4)	1.995(4)	Fe–N(4)	1.998(8)	1.992(9)	1.979(8)	1.989(5)
Imine N						
	Fe–N(2)	1.952(4)	Fe–N(2)	1.932(8)	1.923(8)	1.95(1)	1.917(5)
	Fe–N(3)	1.952(4)	Fe–N(3)	1.939(8)	1.916(8)	1.933(8)	1.912(5)
			Fe–N(5)	1.953(8)	1.949(8)	1.93(1)	1.934(5)
Acetonitrile N						
	Fe–N(5)	1.941(5)	Fe–N(6)	1.963(9)	1.973(9)	1.942(9)	1.950(6)
	Fe–N(6)	1.937(5)					
py–Fe–imine						
	N(1)–Fe–N(2)	83.2(2)	N(1)–Fe–N(2)	80.9(4)	81.1(3)	81.4(4)	80.4(2)
	N(3)–Fe–N(4)	82.6(2)	N(3)–Fe–N(4)	82.0(4)	80.1(4)	80.9(4)	81.1(2)
			N(1)–Fe–N(5)	167.8(4)	170.7(4)	167.0(4)	167.6(2)
			N(2)–Fe–N(4)	166.5(4)	167.3(4)	165.5(3)	168.0(2)
imine–Fe–imine						
	N(2)–Fe–N(3)	93.1(2)	N(2)–Fe–N(3)	87.0(4)	88.3(4)	88.0(4)	88.9(2)
			N(2)–Fe–N(5)	88.9(4)	89.9(3)	88.3(4)	88.0(2)
			N(3)–Fe–N(5)	86.7(4)	87.1(3)	85.9(4)	86.5(2)
py–Fe–py						
	N(1)–Fe–N(4)	102.0(2)	N(1)–Fe–N(4)	93.1(3)	94.8(4)	91.7(4)	94.3(2)
py–Fe–imine						
	N(1)–Fe–N(3)	171.6(2)	N(1)–Fe–N(3)	99.5(3)	95.2(3)	101.6(4)	97.4(2)
			N(1)–Fe–N(5)	167.8(4)	170.7(4)	167.0(4)	167.6(2)
	N(4)–Fe–N(2)	171.6(2)	N(4)–Fe–N(2)	166.5(4)	167.3(4)	165.5(3)	168.0(2)
			N(4)–Fe–N(5)	98.2(4)	94.5(3)	100.0(4)	97.9(2)
py–Fe–MeCN						
	N(1)–Fe–N(5)	90.9(2)	N(1)–Fe–N(6)	87.8(3)	88.1(3)	87.2(4)	87.0(2)
	N(1)–Fe–N(6)	87.3(2)	N(4)–Fe–N(6)	96.2(4)	95.2(4)	96.2(4)	95.7(2)
	N(4)–Fe–N(5)	87.3(2)					
	N(4)–Fe–N(6)	90.6(2)					
imine–Fe–MeCN						
	N(2)–Fe–N(5)	86.0(2)	N(2)–Fe–N(6)	95.7(3)	96.6(4)	96.2(4)	94.8(2)
	N(2)–Fe–N(6)	96.3(2)	N(3)–Fe–N(6)	172.6(3)	174.4(3)	170.8(4)	174.7(2)
	N(3)–Fe–N(5)	96.4(2)	N(5)–Fe–N(6)	86.4(4)	90.3(3)	86.0(4)	89.7(2)
	N(3)–Fe–N(6)	85.6(2)					
MeCN–Fe–MeCN						
	N(5)–Fe–N(6)	176.8(2)					
Imines						
	N(2)–C(7)	1.280(6)	N(2)–C(7)	1.30(1)	1.28(1)	1.24(1)	1.268(9)
	N(3)–C(9)	1.272(6)	N(3)–C(9)	1.28(1)	1.26(1)	1.27(1)	1.270(8)
			N(5)–C(18)	1.29(1)	1.26(1)	1.30(1)	1.279(8)
	Fe–N(2)–C(6)	113.6(3)	Fe–N(2)–C(6)	113.9(6)	112.6(6)	113.3(8)	112.9(4)
	Fe–N(2)–C(7)	128.4(4)	Fe–N(2)–C(7)	121.1(6)	122.0(6)	123.3(8)	122.2(4)
	C(6)–N(2)–C(7)	116.8(4)	C(6)–N(2)–C(7)	123.3(8)	123.8(8)	123(1)	123.2(5)
	Fe–N(3)–C(9)	128.5(4)	Fe–N(3)–C(9)	123.7(7)	121.6(6)	122.4(8)	122.2(4)
	Fe–N(3)–C(10)	112.4(3)	Fe–N(3)–C(10)	112.5(6)	113.0(5)	113.8(7)	113.5(4)
	C(9)–N(3)–C(10)	118.3(4)	C(9)–N(3)–C(10)	122.7(8)	124.5(8)	123(1)	123.5(5)

* Atomic labels correspond to those of molecule **A**.

the following thermodynamic parameters were obtained: $\Delta H = 26$ kJ mol^{-1}, $\Delta S = 73$ J K^{-1} mol^{-1} and $T_c = 351$ K.

Synthesis of complexes 2

A variety of nitriles such as acetonitrile, propionitrile, iso-butyronitrile, benzyl cyanide, benzonitrile, and fluorobenzo-nitriles was found to react with complex **1** at room temperature or at 40 °C on addition of triethylamine to yield iron(II) complexes containing a new series of pentadentate ligands. Formation of a C–C bond between the central carbon of the 1,3-diimine group and the carbon atom of the nitrile occurred. The reaction is presumably preceded by substitution of acetonitrile
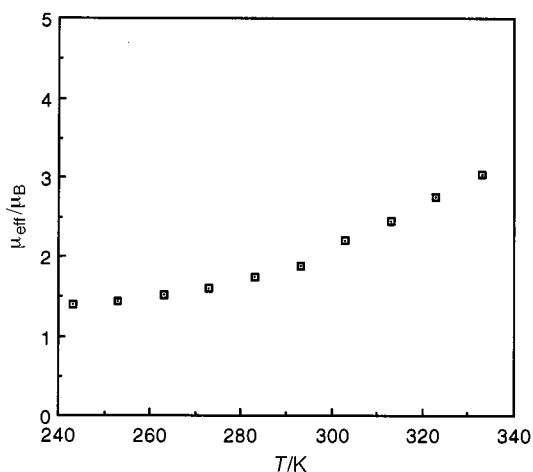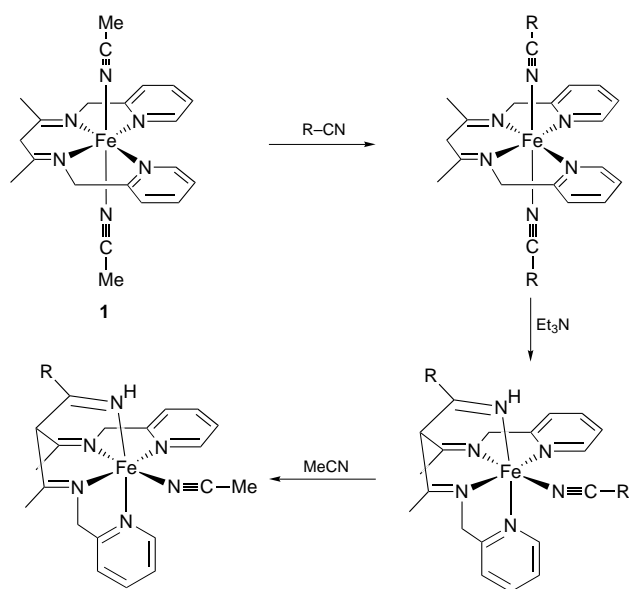
Fig. 4 Plot of the effective magnetic moment (μ_{eff}) of a solution of complex **1** as a function of temperature

Scheme 1

R = Me **2a**, Et **2b**, Pr^i **2c**, PhCH$_2$ **2d**, Ph **2e**, 4-FC$_6$H$_4$ **2f**, 3,4-F$_2$C$_6$H$_3$ **2g**, C$_6$F$_5$ **2h**

Fig. 5 Schematic drawing of complex **2a** and atom labelling
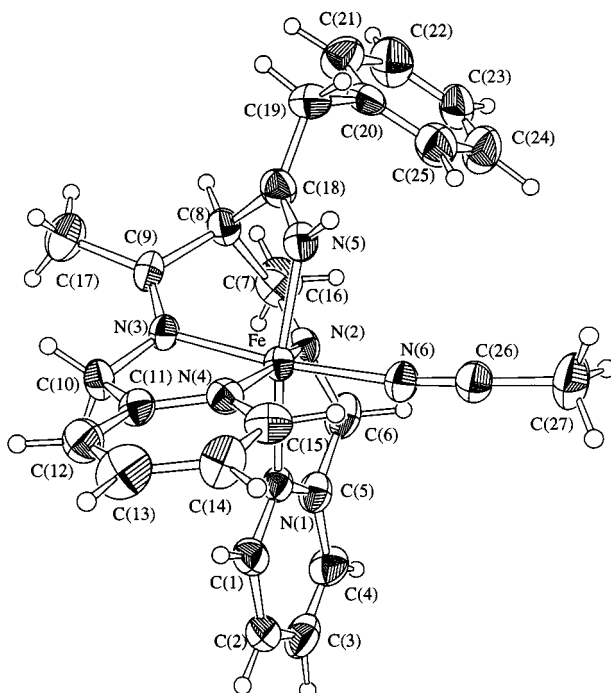
Fig. 6 Perspective view of [FeL^{2d}(MeCN)][PF$_6$]$_2$·Me$_2$CO with 30% thermal ellipsoids for non-hydrogen atoms

with solvent nitrile to form bis(solvent nitrile) complexes. The isolated complexes were redissolved in acetonitrile and the addition of thf or ether caused precipitation of crystals of complexes **2a**–**2h** as shown in Scheme 1. Several attempts to prepare the nitrile adduct from pivalonitrile by this method, however, were unsuccessful.

Structures of complexes 2a, 2d, and 2e

In order to confirm and characterize the structures of the iron(II) complexes with the newly formed pentadentate ligands, X-ray crystallography was carried out. Final positional parameters for **2a** had been deposited earlier.[16] For **2a** there are two crystallographically independent molecular ions (**A** and **B**) with almost identical structures as seen in Table 3, where the selected bond distances and angles of **2a**, **2d**, and **2e** are compared with those of **1**.

The structure of complex **2a** is shown schematically in Fig. 5 with atom labelling and those of **2d** and **2e** are in Figs. 6 and 7 respectively. These four structures show common features: the parent tetradentate ligand (L^1) changes its co-ordination mode from *trans* to *cis*-β, and the nitrile is fused to the central carbon atom of the 1,3-diimine group yielding a C–C(R)=NH group,
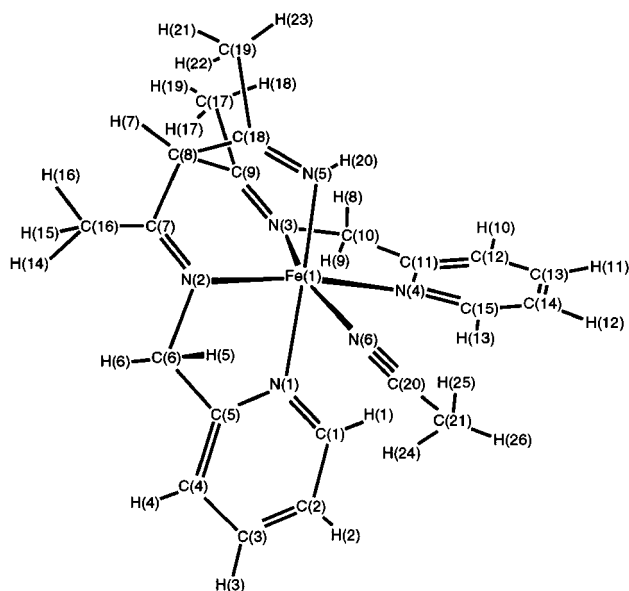
where R = Me, benzyl and phenyl for **2a**, **2d** and **2e** respectively. Thus, in all four structures each central iron(II) is wrapped by the pentadentate ligands L^{2a}, L^{2d} and L^{2e}, which have three isolated imines attached to C(8). The conformation of the 1,3-diimine group changes from planar to boat due to the bridging alkyl- or aryl-methylimine. The carbon atom C(8) of **2d** is located 1.57 Å above the plane defined by Fe, N(2), N(3), N(4) and N(6). The flanking carbon atoms, C(7) and C(9), also deviate in the same direction by 0.54 and 0.88 Å respectively. The C=N bond distances are in the range expected for localized imines and the angles around the carbon and nitrogen atoms of those imines do not deviate significantly from 120° as seen in Table 3.

The conformational restriction caused by tethering with the methylimine bridge may account for the preference of a non-planar co-ordination compared to the planar co-ordination of the parent tetradentate ligand L^1, because the two hydrogens at
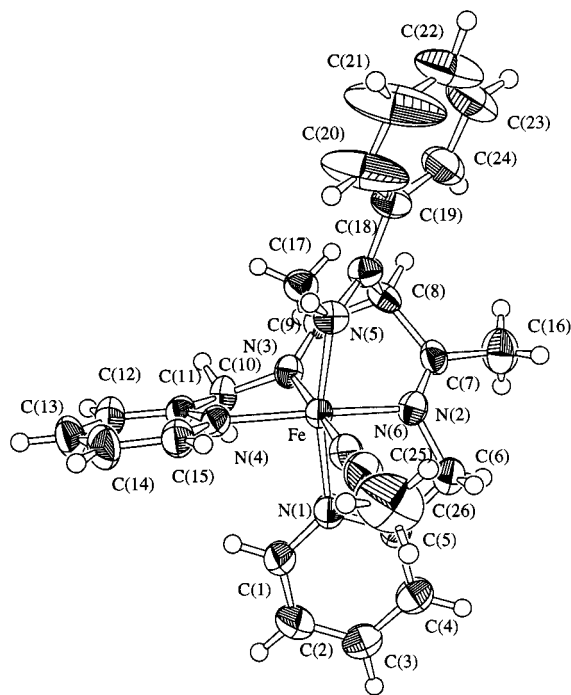
Fig. 7 Perspective view of complex **2e** with 50% thermal ellipsoids for non-hydrogen atoms

Fig. 8 Proton NMR spectra of complex **2a** in CD$_3$CN

Fig. 9 The HMBC spectrum of a CD$_3$CN solution of complex **2a** at −10 °C

the 6 positions of the pyridine rings would be brought close together in the latter situation. The sixth co-ordination site *trans* to the imine nitrogen, N(3) for **2a**, **2d** and **2e**, is occupied by an acetonitrile molecule. The N−Fe−N bond angles for the five-membered chelate rings are narrower (80.1–82.0°) for **2a**, **2d** and **2e** than those found for **1** (82.6 and 83.2°).

One trigonal face of the octahedral structure is occupied by the three isolated imines which are linked to the tetrahedral C(8). The imine bonds in each molecule are parallel to each other and also to the axis passing through Fe and C(8). These triimine cores are similar in exhibiting right angles for the N$_{imine}$−Fe−N$_{imine}$ bond angles to the core reported for *cis*[3,11-bis(1-iminoethyl)-2,12-dimethyl-1,5,9,13-tetraazacyclohexa-deca-1,4,9,12-tetraene]iron(II) hexafluorophosphate where the hexadentate ligand is formed by the addition of acetonitrile to the macrocyclic tetraimine involving a 1,3-diimine group.[13]

The two pyridine rings co-ordinate in *cis* position to each other and the dihedral angles between the pyridine planes are 80.9–85.3, 88.53 and 85.97° for complexes **2a**, **2d** and **2e**. One pyridine nitrogen N(1) is located at the apical and the other N(4) is on the same plane with respect to the six-membered 1,3-diimine chelate ring. For **2d** the dihedral angles Fe−N(2)−C(6)−C(5) [29.6(9)°] and Fe−N(3)−C(10)−C(11) [28.5(9)°] are similar to each other, but the dihedral angle C(7)−N(2)−C(6)−C(5) [138.9(9)°] is opposite in sign to that of C(9)−N(3)−C(10)−C(11) [−143.2(9)°]. This difference accounts for the different co-ordination modes of the pyridine rings.

Proton NMR spectra of complexes 2

The iron(II) complexes **2a**–**2h** exhibit temperature-dependent ^{1}H NMR spectra, and one of these is reproduced in Fig. 8. At or above room temperature, the signals were broadened except for one sharp doublet ($J = 1.8$ Hz) around δ 5.68. The spectrum changed to sharp signals at low temperature. Furthermore, when the complex was prepared from CD$_3$CN the spectrum lacked the methyl signal, between the two methyl resonances derived from the L^1 skeleton. The signal that appeared at δ 11.23 for **2a** is attributed to the co-ordinated C=NH group which is consistent with narrow bands observed at 3245 and 3263 cm^{-1} in the infrared spectrum. The HMQC and HMBC spectra[18,19,24] of **2a** at −10 °C shown in Fig. 9 uniquely deter-
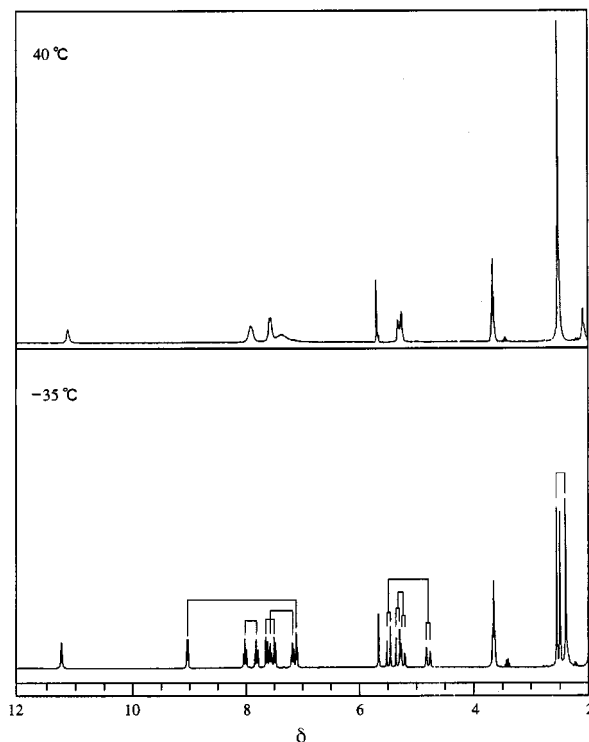
mined the ^{13}C and ^{1}H signals. The hydrogen atom labellings are those shown for the molecular cation **2a** in the Fig. 5. Based on the X-ray crystallographic data described above, H(1) is assigned as the hydrogen atom attached to the apical pyridine ring. Two pairs of methylene protons [H(5) and H(6), H(8) and H(9)] exhibit AB quartets with $J = 17.4$ Hz. The former have chemical shifts of δ 5.25 and 5.48 and the latter δ 5.33 and 4.82 respectively for **2a**. The bridgehead methine proton has its resonance at δ 5.68.
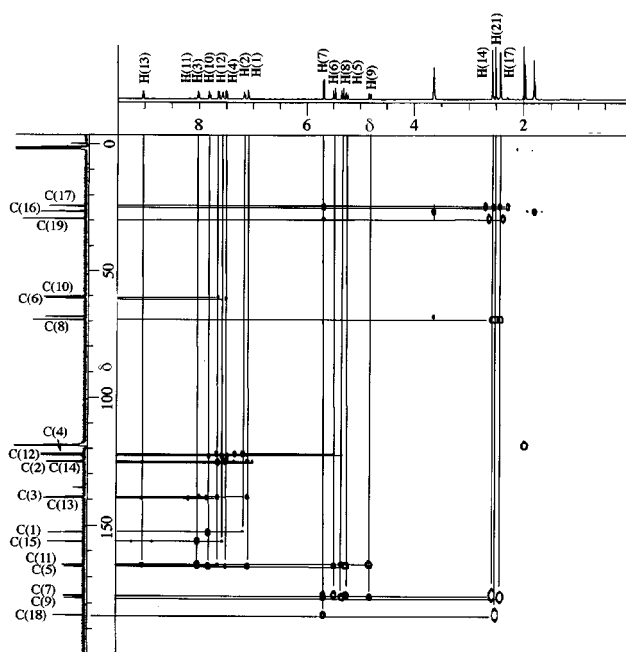
At low temperatures the ^{1}H NMR spectra of complexes **2b**–**2h** showed that two pyridyl groups and the two methyl groups are unsymmetrical and the chemical shifts at −35 °C are almost same as those for **2a** and are assigned as in Table 1. Each proton
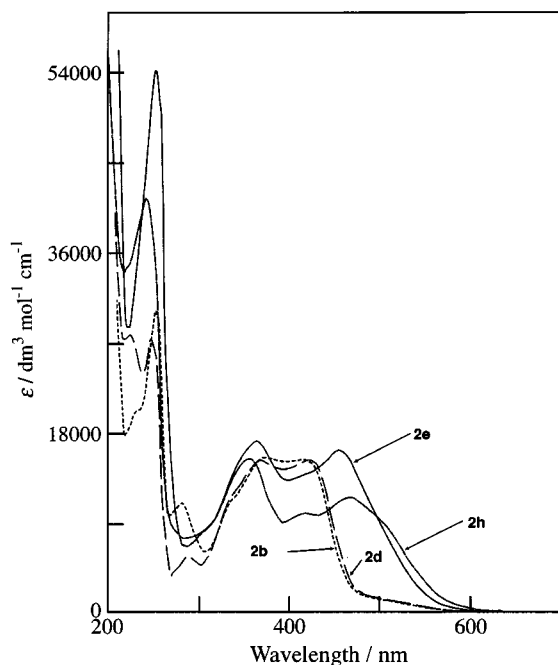
Fig. 10 Selected UV/VIS spectra of the nitrile adducts

on the pyridine rings has almost the same chemical shift irrespective of the change in substituent on the methylimine moiety in the nitrile adducts. Proton H(1) of the pyridine ring is shifted upfield compared to the corresponding H(13) of the other pyridine ring. The upfield shift arises presumably from the ring-current effect of the other pyridine ring. A strong dependency on the nitrile employed is seen for H(20): C=NH resonates at δ 13.18 for complex **2h** and at δ 11.04 for **2b** reflecting the resonance effect of the substituent of the nitrile.

Most signals of complexes **2** were broadened above 0 °C, and appeared as sharp signals again at 40 °C, see Fig. 8. The signals at 40 °C appeared at chemical shifts averaged between those of the signals at −35 °C. The analysis of the temperature dependency showed that the pairs linked by lines in Fig. 8 merged to give the time-averaged signal at higher temperature.

Other spectroscopic properties of complexes 2

Representative absorption spectra of acetonitrile solutions of the iron(II) complexes are shown in Fig. 10. In the visible region the spectra of **2b** and **2d** presented one shoulder and a broad band around 430 and 460 nm, attributable to charge transfer. The energy difference between these two transitions is around $\Delta E = 1520$ cm^{-1} very near the imine charge-transfer (CT) transition of 1530 cm^{-1} reported by Nakamoto and co-workers.[26] The transitions at 240 and 280 nm are attributable to pyridine rings. The adducts with aromatic nitriles showed one or two absorption bands at wavelengths longer than 450 nm. The CT transitions from Fe^{II} to monoimine and pyridine have been reported to be located at 320 and 340–420 nm respectively[26] and iron(II) complexes with the hexadentate ligands derived from macrocyclic tetramines and acetonitrile have been reported to give bands at 415–423 (ε = 7000–10 000) and 292–299 nm (ε = 3500–5100 dm^3 mol^{-1} cm^{-1}).[12]

Electrochemical properties

The cyclic voltammograms of complexes **2a**, **2b** and **2d–2h** were recorded at room temperature. All showed one reversible anode and cathode peaks with i_{pa}/i_{pc} near to unity and ΔE 60 to 70 mV. Their redox potentials fall in the range 0.50 to 0.75 V $vs.$ Ag–Ag$^+$: **2a**, 0.52; **2b**, 0.52; **2d**, 0.56; **2e**, 0.55; **2f**, 0.58; **2g**, 0.61; **2h**, 0.74 V. Thus the iron(II) complexes can be oxidized to iron(III) reversibly.

Discussion

The tetradentate compound L^1 is formally obtained from the condensation between one molecule of pentane-2,4-dione and two of 2-aminomethylpyridine. Up to the present time, however, we have not succeeded in isolating it. Although complex **1** can also be prepared by the reaction of iron(II) perchlorate with a 1:2 mixture of pentane-2,4-dione and 2-aminomethylpyridine under dry conditions, the method described in the Experimental section normally gives reproducible results. The ^{1}H NMR spectrum of tridentate, 4-oxo-2-pentylidene-2-pyridylmethanamine, obtained by condensation of pentane-2,4-dione and 2-aminomethylpyridine, revealed the enol form. The formation of L^1, therefore, occurs only in the presence of a template metal ion.

With the use of hexa(acetonitrile)iron(II) prepared *in situ* as a template, the bis(acetonitrile)iron(II) complex of L^1 was obtained at room temperature and isolated as red crystals (**1**). The reaction conditions had to be controlled by the use of a restricted amount of 2-aminomethylpyridine so that the medium did not become basic. This precaution prevented any succeeding reaction from occurring.

The addition of triethylamine to a red nitrile-containing solution of complex **1** caused a change to intense orange at room temperature or at 40 °C. Addition of ether or thf facilitated isolation of the reaction product, **2**, as depicted in Scheme 1. Each product showed a ^{1}H NMR spectrum which corresponded to the formation of an iron(II) complex with a new pentadentate ligand derived from the addition of a nitrile to the central carbon atom of the 1,3-diimine core of L^1. The ^{1}H NMR spectra are similar, suggesting that the structures of complexes **2** do not vary with the nitriles employed, as was confirmed by the crystal structure determinations of three of them.

The addition of acetonitrile to a 1,3-diimine group has been previously reported by Riley *et al.*[12] for 15- or 16-membered macrocyclic tetraimines. The use of triethylamine to neutralize the macrocyclic tetraiminium methanesulfonate in acetonitrile resulted in the formation of acetonitrile adducts and prevented the presumed precursor bis(nitrile)iron(II) from being isolated. On the other hand, here the restricted use of base has allowed the isolation of complex **1**, the application of which to the reaction with other nitriles yielded a series of iron(II) complexes with L^{2a}–L^{2h}.

One probable reaction mechanism involves nucleophilic attack of the carbanion formed at the central carbon of the 1,3-diimine group either on the acetonitrile co-ordinated at the apical position and activated by the iron(II) centre as proposed by Riley *et al.*,[12] or on a bulk acetonitrile molecule followed by co-ordination of the formed imine nitrogen to the apical position.

The new iron(II) complexes, **1** and **2**, have been shown to be low spin and to have distorted O_h geometries in crystals at room temperature, because the average Fe–N bond distances are 1.96 and 1.95 to 1.97 Å for **1** and **2**, respectively. Several iron(II) complexes of polydentate ligands having 2-pyridylmethyl arms have previously been reported.[5–9] The Fe–N$_{py}$ distances are shorter for low- (1.94–1.97 Å) than for high-spin complexes (2.21–2.22 Å).[7] The Fe–N$_{py}$ distances in **1** and **2** are slightly longer than those for low-spin iron(II) complexes: 2.0 Å for **1** and 1.98 to 2.00 Å for **2**. The reasons for this are presumably different for **1** and **2**. For **1** the tetradentate ligand occupies a co-ordination plane, and planar rearrangement would exert an intramolecular repulsion between the two hydrogens attached to positions 6 of the pyridines. The two pyridine rings swing away from each other, dihedral angle 30.95°,[16] in order to decrease the intramolecular repulsion. Similar interligand repulsion has been reported for [Pd(bpy)$_2$][NO$_3$]$_2$·H$_2$O where the dihedral angle between the bipyridine planes is 33°.[27] This deformation can be compensated by the elongation of the
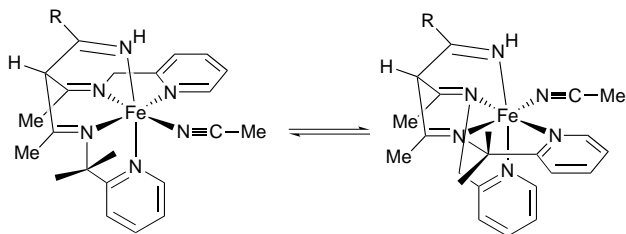
Scheme 2 The isomerization of complex **2**

Fe–N_{py} distances, supported by slight widening of the N_{py}–Fe–N_{py} bond angle. In complexes **2**, the dihedral angles between the two pyridine rings are about 90° and no intramolecular repulsion is observed between these rings, but the shorter Fe–N_{imine} bond distances and the rigid triimine core cause elongation of the Fe–N_{py} bond. The Fe–$N_{nitrile}$ distances are the shortest of the Fe–N bonds in **1**, *i.e.* 1.94 Å. This value is similar to those found for other *trans*-bis(acetonitrile)(macrocyclic amine)iron(II) complexes.[28] The Fe–$N_{nitrile}$ bond is slightly longer (1.95–1.97 Å) for **2** due to the presence of the triimine core.

The ^{1}H NMR spectra of complexes **1** and **2** showed temperature dependences of different natures. For **1** the chemical shift of each signal moves away from that expected for a diamagnetic compound above 20 °C. A similar change has been reported for [*N*,*N*,*N*′,*N*′-tetrakis(2-pyridylmethyl)ethane-1,2-diamine]-iron(II) by Chang *et al.*[9] This behaviour is consistent with a spin equilibrium between $^1A_{1g}$ and $^5T_{2g}$ electronic configurations[8,9] as confirmed by magnetic susceptibility measurements. Van't Hoff plots of μ_{eff} between 20 and 60 °C gave the ΔH and ΔS for $^1A_{1g} \longrightarrow {}^5T_{2g}$ as 25.7 kJ mol^{-1} and 73.1 J K^{-1} mol^{-1}, respectively, which are typical values for spin interconversion of iron(II) complexes with pyridylmethyl-substituted ligands.[8,9,29] Furthermore, the absorption intensity at 527 nm decreased as the temperature was raised. The proton most susceptible to temperature change is that at the 6 position of the pyridine rings. The number of signals, which was unchanged between 20 and −50 °C, increased at −60 °C confirming the presence of *trans*- and *cis*-β isomers. This phenomenon shows that **1** undergoes rapid interconversion between the two isomers above −50 °C.

The ^{1}H NMR spectra of complexes **2** showed sharp signals below −10 °C, and their number revealed that the complexes have asymmetrical structures as confirmed by X-ray crystallography. Above room temperature, however, time-averaged signals were observed. The methine proton, H(7), was observed as a sharp signal irrespective of temperature. These changes are attributable to an isomerization as shown in Scheme 2 in which the two pyridine rings exchange their co-ordination sites and the acetonitrile changes its site simultaneously.[9,30]

The largest chemical shift differences are found for the pairs H(1) and H(13) (1.93 ppm) and C(1) and C(15) (3.50 ppm). The H(1) and C(1) resonances are upfield shifted, attributable to the ring-current effect of the pyridine rings: H(1) is located above the pyridine ring in the planar co-ordination arrangement and the distances between it and the centre of the pyridine ring are 3.0 and 3.1 Å and the azimuthal angles are 30 and 35° for molecules **A** and **B** of complex **2a**. These geometrical values result in an upfield shift of 0.9 to 1.3 ppm if the parameters for pyridine are assumed to be the same as those for benzene.[31] This assumption was in fact employed to assign the upfield signal to H(1). Two methylene groups appeared, both as AB quartets, and the doublets at higher field were broader than those at lower field due to the ^5J homoallyl coupling with CH_3 as confirmed by irradiation of the methyl groups.

The UV/VIS spectrum of complex **1** in acetonitrile solution resembles that of bis(acetonitrile)(5,14-dimethyl-1,4,8,11-tetraazacyclotetradeca-4,6,11,13-tetraene)iron(II)[12] in having two absorption maxima at 527 (18 980) and 720 nm (13 890
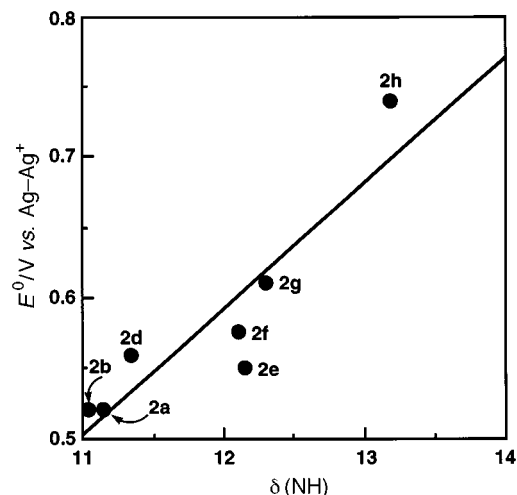

Fig. 11 Correlation between the redox potential and the chemical shift of C=N*H* for various nitrile adducts

cm^{-1}), *cf.* 469 and 730 nm for the latter. These maxima have been assigned to $^1A_{1g} \longrightarrow {}^1E_g$ and $\longrightarrow {}^1A_{2g}$ transitions under D_{4h} symmetry.[12] Based on the energies of the two bands in a first-order approximation given by Wentworth and Piper[32] and $Dq^z \approx 940$ cm^{-1} for acetonitrile,[12] Dq^{xy} is estimated to be 1960 cm^{-1} for the open-chain L^1 ligand which decreased considerably from 2400 cm^{-1} for the macrocyclic tetraamine.[12] These values show that the ligand-field stabilization energy for the open-chain L^1 ligand is slightly weaker than that for the macrocyclic tetraimine.

The absorption bands in the visible region of complexes **2** did not show the d–d transitions due to the strong overlap of charge-transfer bands. The nature of the latter bands is difficult to delineate because the presence of the pyridine rings complicates the spectral features.

The reduction potentials of the Fe$^{II/III}$ couple of complexes **2** indicate that the electron-withdrawing substituent of the nitriles raises the potential. The chemical shifts of C=N*H* revealed a strong dependency on the substituent: an electron-withdrawing substituent reduces the electron density around the proton nucleus and deshields it. The relationship between the redox potential and the chemical shifts shown in Fig. 11 is not strict because the substituent effect on the redox potential arises through both σ donation and π-back donation.[33]

References

1 M. J. Blandamer, J. Burgess, R. I. Haines, F. M. Mekhail and P. Askalani, *J. Chem. Soc., Dalton Trans.*, 1978, 1001.

2 A. Earnshaw, E. A. King and L. F. Larkworthy, *J. Chem. Soc. A*, 1968, 1048.

3 V. L. Goedken, *J. Chem. Soc., Chem. Commun.*, 1972, 207; A. M. C. Ferreira and H. E. Toma, *J. Chem. Soc., Dalton Trans.*, 1983, 2051; M. Goto, M. Takeshita, N. Kanda, T. Sakai and V. L. Goedken, *Inorg. Chem.*, 1985, **24**, 582; M. Goto, N. Koga, Y. Ohse, H. Kurosaki, T. Komatsu and Y. Kuroda, *J. Chem. Soc., Chem. Commun.*, 1994, 2015.

4 V. L. Goedken and D. H. Busch, *J. Am. Chem. Soc.*, 1972, **94**, 7355; K. Pohl, K. Wieghardt, W. Kaim and S. Steenken, *Inorg. Chem.*, 1988, **27**, 440.

5 S. M. Nelson and J. Rodgers, *J. Chem. Soc. A*, 1968, 272; R. Butcher and A. W. Addison, *Inorg. Chim. Acta*, 1989, **158**, 211.

6 Yu-Min Chiou and Lawrence Que, jun., *J. Am. Chem. Soc.*, 1995, **117**, 3999.

7 Yan Zang, J. Kim, Yanhong Dong, E. C. Wilkinson, E. H. Appelman and Laurence Que, jun., *J. Am. Chem. Soc.*, 1997, **119**, 4197.

8 H. Toftlund and S. Yde-Andersen, *Acta Chem. Scand.*, *Ser. A*, 1981, **35**, 575; J. K. McCusker, K. N. Walda, R. C. Dunn, J. D. Simon, D. Magde and D. N. Hendrickson, *J. Am. Chem. Soc.*, 1993, **115**, 298; J. K. McCusker, H. Toftlund, A. L. Rheingold and D. N. Hendrickson, *J. Am. Chem. Soc.*, 1993, **115**, 1797.

9 Hsiu-Rong Chang, J. K. McCusker, H. Toftlund, S. R. Wilson, A. X. Trautwein, H. Winkler and D. N. Hendrickson, *J. Am. Chem. Soc.*, 1990, **112**, 6814.

10 D. A. Buckingham, B. M. Foxman, A. M. Sargeson and A. Zanella, *J. Am. Chem. Soc.*, 1972, **94**, 1007; D. A. Buckingham, F. R. Keene and A. M. Sargeson, *J. Am. Chem. Soc.*, 1973, **95**, 5649; K. B. Nolan and R. W. Hay, *J. Chem. Soc.*, *Dalton Trans.*, 1974, 914; A. W. Zanella and P. C. Ford, *Inorg. Chem.*, 1975, **14**, 42; D. A. Buckingham, P. Morris, A. M. Sargeson and A. Zanella, *Inorg. Chem.*, 1977, **16**, 1910; W. R. Ellis and W. L. Purcell, *Inorg. Chem.*, 1982, **21**, 834; D. A. Buckingham, C. R. Clark, B. M. Foxman, G. J. Gainsford, A. M. Sargeson, M. Wein and A. Zanella, *Inorg. Chem.*, 1982, **21**, 1986; N. J. Curtis and A. M. Sargeson, *J. Am. Chem. Soc.*, 1984, **106**, 625; F. Scavo and P. Helquist, *Tetrahedron Lett.*, 1985, **26**, 2603; P. Paul and K. Nag, *Inorg. Chem.*, 1987, **26**, 2969; L. Roecker, A. M. Sargeson and A. C. Willis, *J. Chem. Soc.*, *Chem. Commun.*, 1988, 119; W. Schulz, H. Pracejus and G. Oehme, *Tetrahedron Lett.*, 1989, **30**, 1229; A. Syamala and A. Chakravarty, *Inorg. Chem.*, 1991, **30**, 4699; J. Grigg, D. Collison, C. D. Garner, M. Helliwell, P. A. Tasker and J. M. Thorpe, *J. Chem. Soc.*, *Chem. Commun.*, 1993, 1807.

11 K. Bowman, D. P. Riley, D. H. Busch and P. W. R. Corfield, *J. Am. Chem. Soc.*, 1975, **97**, 5036; D. P. Riley and D. H. Busch, *Inorg. Chem.*, 1983, **22**, 4141; D. P. Riley, J. A. Stone and D. H. Busch, *J. Am. Chem. Soc.*, 1977, **99**, 767; D. P. Riley and D. H. Busch, *Inorg. Chem.*, 1983, **22**, 4141.

12 D. P. Riley, J. A. Stone and D. H. Busch, *J. Am. Chem. Soc.*, 1976, **98**, 1752.

13 K. B. Mertes, P. W. R. Corfield and D. H. Busch, *Inorg. Chem.*, 1977, **16**, 3226.

14 W. C. Weiss and V. L. Goedken, *J. Am. Chem. Soc.*, 1976, **98**, 1752; M. C. Weiss, G. C. Gordon and V. L. Goedken, *J. Am. Chem. Soc.*, 1979, **101**, 857.

15 F. Mizukami, K. Satoh, S. Niwa, T. Tsuchiya, K. Shimizu and J. Imamura, *Sekiyu Gakkai Shi*, 1985, **28**, 293.

16 M. Goto, Y. Ishikawa, T. Ishihara, C. Nakatake, T. Higuchi, H. Kurosaki and V. L. Goedken, *Chem. Commun.*, 1997, 539.

17 TEXSAN program system, Molecular Structure Corporation, Houston, TX, 1985 and 1992.

18 A. Bax and S. Subramanian, *J. Magn. Reson.*, 1986, **67**, 565.

19 A. Bax and M. F. Summers, *J. Am. Chem. Soc.*, 1986, **108**, 2093.

20 D. F. Evans, *J. Chem. Soc.*, 1959, 2003.

21 O. Kahn, *Molecular Magnetism*, VCH, Weinheim, 1993, p. 4.

22 S. O. Wandiga, J. E. Sarneski and F. L. Urbach, *Inorg. Chem.*, 1972, **11**, 1349.

23 L. L. Martin, K. S. Hagen, A. Hauser, R. L. Martin and A. M. Sargeson, *J. Chem. Soc.*, *Chem. Commun.*, 1989, 2003.

24 A. Bax, R. H. Griffey and B. L. Hawkins, *J. Magn. Reson.*, 1983, **55**, 301; G. Otting and K. Wuthrich, *J. Magn. Reson.*, 1988, **76**, 569; A. Bax and D. Marion, *J. Magn. Reson.*, 1988, **78**, 186.

25 J. C. Dabrowiak and D. H. Busch, *Inorg. Chem.*, 1975, **14**, 1881.

26 R. J. H. Clark, P. C. Turtle, D. P. Strommen, B. Streusend, J. Kincaid and K. Nakamoto, *Inorg. Chem.*, 1977, **16**, 84.

27 A. J. Carty and P. C. Chieh, *J. Chem. Soc.*, *Chem. Commun.*, 1972, 158; M. Hinamoto, S. Ooi and H. Kuroya, *J. Chem. Soc.*, *Chem. Commun.*, 1972, 356.

28 H. W. Smith, B. D. Santasiero and E. C. Lingafelter, *Cryst. Struct. Commun.*, 1979, **8**, 49; L. E. McCandlish, B. D. Santassiero, N. J. Rose and E. C. Lingafelter, *Acta Crystallogr.*, *Sect. B*, 1979, **35**, 3053; V. L. Goedken, Y.-E. Park, S. M. Peng and J. Molin-Norris, *J. Am. Chem. Soc.*, 1974, **96**, 7693.

29 J. P. Jesson, S. Trofimenko and D. R. Eaton, *J. Am. Chem. Soc.*, 1967, **89**, 3158; M. A. Hoselton, L. J. Wilson and R. S. Drago, *J. Am. Chem. Soc.*, 1975, **97**, 1722; H. L. Chum, J. A. Vanin and M. I. D. Holanda, *Inorg. Chem.*, 1982, **21**, 1146.

30 R. G. Wilkins, *The Study of Kinetics and Mechanism of Reactions of Transition Metal Complexes*, Allyn and Bacon, Boston, 1974, ch. 7.

31 R. J. Abraham, S. C. M. Fell and K. M. Smith, *Org. Magn. Reson.*, 1977, **9**, 367.

32 R. A. D. Wentworth and T. S. Piper, *Inorg. Chem.*, 1965, **4**, 709.

33 S. S. Fielder, M. C. Osborne, A. B. P. Lever and W. J. Pietro, *J. Am. Chem. Soc.*, 1995, **117**, 6990.